Processing a class of ophthalmological images using an anisotropic diffusion equation

Andrew P. Papliński
Computer Science and Software Engineering
Monash University, Australia
app@csse.monash.edu.au

James F. Boyce
Wheatstone Laboratory
King's College London, U.K.
jfb@physig.ph.kcl.ac.uk

Abstract

In this paper we discuss application of an anisotropic diffusion equation in processing Posterior Capsular Opacification (PCO) Images. Such images are recorded to monitor the state of a patient's vision after cataract surgery. Nonlinear filtering using an anisotropic diffusion equation generates segmentation-like results by enhancing edges represented by the high value of the gradient and smoothing away small inter-regional features. The algorithm ensures the existence of a stable fixed-point solution and maintains a mean grey level of image intensity.

Keywords: Medical Imaging, Posterior Capsular Opacification, Partial Differential Equations, Anisotropic Diffusion Equation, Segmentation.

1 Introduction

We present an application of partial differential equations (PDEs), more specifically, of an anisotropic diffusion equation in processing Posterior Capsular Opacification (PCO) images which are recorded to monitor the post-cataract-surgery state of patients vision. Our standard method of segmentation such images ([1, 2, 3, 4]) is based on the application of a directional variance operator and co-occurrence arrays. The method works very efficiently in the majority of cases, but there are a non-negligible number of cases where the segmentation error is unacceptably high. In such cases, we demonstrate in this work that an anisotropic diffusion equation applied to the variance image before the segmentation operation is performed reduces the segmentation error significantly.

Our work was influenced by recent considerations on variational methods presented in the IEEE Transaction on Image Processing *Special Issue on Partial Differential Equations* ([5]). Specifically, lots of attention has be recently given to an anisotropic diffusion equation and its applications in image filtering and restoration [6, 7, 8]. Other PDEs, such as heat equations and wave equations have also been studied in the context of image processing.

The formulation of the algorithms presented in this work is based on [6], and on the application in processing the PCO images reported in [9]. This work is also linked to our efforts (reported in [10]) related to the application of the first order wave equation to model some aspects of an underlying biological process, namely the movement of concentration of epithelial cells. Proliferation of these cells is believed to be responsible for the posterior capsular opacification.

2 Brief description of PCO images

The condition of eye lens cataract is ultimately treated by surgery when the patient's natural lens is replaced by an intra-ocular plastic implant [11]. A common post-surgical complication is opacification of the eye's posterior capsule [12, 13]. It can be assumed that Posterior Capsular Opacification is caused by the proliferation of epithelial cells across the back surface of the capsule. This process obscures the implanted lenses and is responsible for deterioration of patients vision. The opacification is monitored by recording images of the back-surface of the implant at regular intervals after surgery [12, 13].

Examples of two PCO images recorded two years after an operation are given in Figure 1. Such images are characteristic of patients with very impaired vision. The diameter of the implanted lens is approximately 6mm, and the image size is in the range of 900×900 pixels, which results in a resolution of approximately 7 pixels per μm. The total size of the raw image frame is 1536×1024. Note the Purkunje reflection spots from the cornea and the anterior surface of the implanted lens. The intensity range is 8 bits.

The Department of Ophthalmology at St. Thomas' Hospital, London and the Image Processing Group from King's College London have developed a software pack-

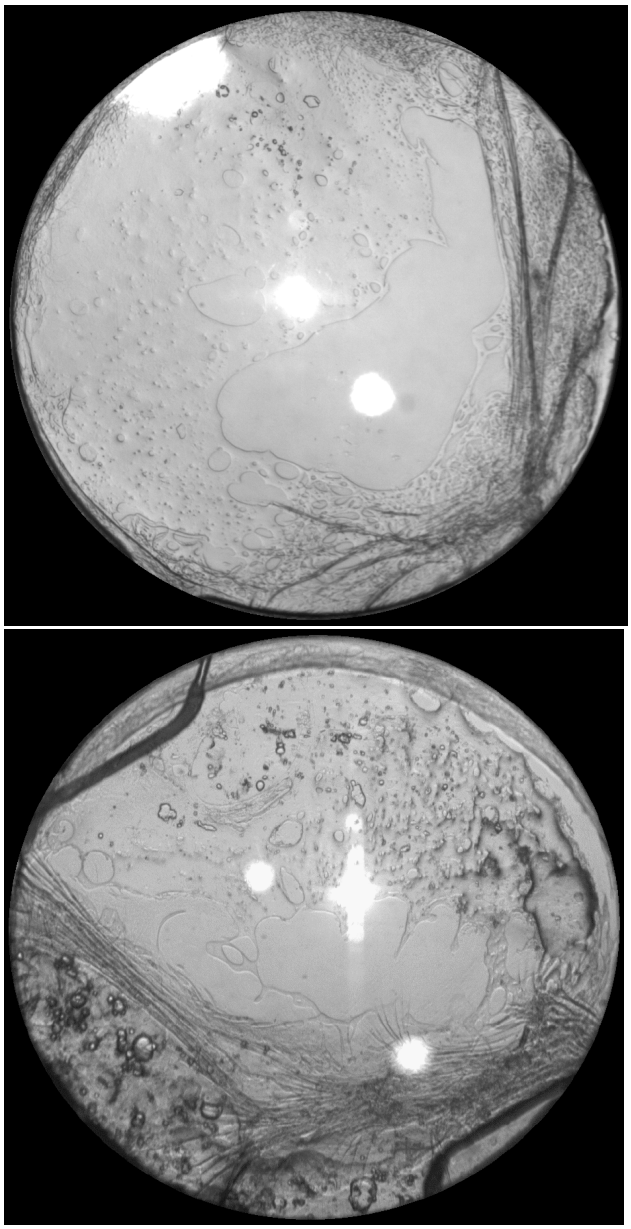

Figure 1: Two pre-processed two-year PCO images of patients with defined impaired vision

age to assist in the automatic evaluation of posterior capsular opacification and, ultimately, patient's visual acuity. For details the reader is referred to [1, 2, 4, 11]. This paper describes ongoing work on improving and enriching methods of interpretation of PCO images. Specifically, we concentrate on images which are difficult to segment using our tools based of the directional variance operator and co-occurrence arrays. Areas of low variance will be, in general, classified as representing transparent regions of the posterior capsule, whereas high variance indicates opaque regions. An example of such a difficult-to-segment image is given in Figure 1 (the top image) where there are areas of small variance, as in the upper left corner of the image, which can be confused with transparent regions, like the one in the central part of the image.

3 Filtering using an anisotropic diffusion equation

An anisotropic diffusion equation in its standard form can be presented as:

$$\frac{\partial u(\mathbf{x},t)}{\partial t} = \mathrm{div}(L(\mathbf{x},t)\nabla u(\mathbf{x},t)) \tag{1}$$

where $u(\mathbf{x},t)$ is an evolving image intensity, ∇u is its gradient, and $L(\mathbf{x},t)$ is a 2×2 diffusion matrix responsible for anisotropy. The diffusion equation describes an image change which is proportional to a sum of spatial derivatives of the diffusion vector, $v = L \cdot \nabla u$. In particular, when the diffusion vector becomes zero, the image intensity reaches its steady state.

Following [6] we exploit two basic ideas which are important from the point of view of obtaining segmentation-like behaviour of the algorithm based on eqn (1). The first idea is that the anisotropy vector should steadily reach the value of zero, and the second that such state is obtained either by the diffusion matrix being the orthogonal projection of the image gradient which gives $L \cdot \nabla u = 0$, or by the image gradient approaching zero. This can be achieved by means of the following relaxation equation:

$$\frac{\partial L(\mathbf{x},t)}{\partial t} + \frac{1}{\tau}L(\mathbf{x},t) = \frac{1}{\tau}F(\nabla u(\mathbf{x},t)) \tag{2}$$

where $F(\nabla u(\mathbf{x},t))$ is a 2×2 anisotropy "force" matrix, and τ is a time constant which determines the speed of relaxation of the diffusion matrix. The diffusion matrix evolves from its initial value to the one enforced by the F matrix. The force matrix, F, will be selected based on the value of of the magnitude of the image gradient. If the image gradient exceeds a threshold parameter, s, then the matrix F will be the orthogonal projection, otherwise its form will ensure isotropic diffusion, which smoothes the image in the areas where the gradient falls below the threshold parameter. More specifically, the selected form of the force function is as follows:

$$F(\nabla u) = \begin{cases} P(\nabla u) & \text{if} \quad r \geq 1 \\ 1.5(1-r^2)I + r^2 P(\nabla u) & \text{if} \quad r < 1 \end{cases} \tag{3}$$

where the projection matrix, $P(\nabla u)$, is an "outer square" of the unit vector orthogonal to the image gradient, namely:

$$P(\nabla u) = \frac{1}{|\nabla u|^2} \begin{bmatrix} g_2 \\ -g_1 \end{bmatrix} \cdot \begin{bmatrix} g_2 & -g_1 \end{bmatrix} \tag{4}$$

where the gradient components are

$$\nabla u = [g_1 \; g_2]$$

and the stiffness ratio, r, is

$$r = \frac{|\nabla u|}{s} \tag{5}$$

s, being the stiffness threshold.

The set of equations (1) ... (5) gives a stable solution to the diffusion equation maintaining strong edges in the image and flattening image features which are considered to be irrelevant. For a rigorous mathematical treatment the reader is referred to [6].

4 Segmentation example

In this section we demonstrate how the anisotropic diffusion equation discussed in the previous section can be used to improve segmentation of a difficult-to-segment PCO image. We use the top image from Figure 1 as a test image. First, we apply to our test image a tri-directional variance operator as presented in [1, 2, 4]. The span of the lobe of the operator is 3, and the lobe overlapping factor is 0.5. The resulting variance image is presented in Figure 2. For purposes of illustration the image in Figure 2 is taken to be the square root of the directional standard deviation operation. This emphasises the areas of relatively low variance (dark areas in the Figure 2), which are prevalent in the image. In addition, images have been down-sampled by the factor of five to reduce the size of related postscript images. Next, for the variance image, we calculate the co-occurrence array from which the segmentation classes can be inferred. The resulting segmented image is shown in Figure 3.

With reference to the top image of Figure 1 it can be observed that the segmentation tools correctly identify the central part of the image (light grey in Figure 3) as representing the transparent section of the posterior capsule. In addition, however, the low-variance areas in the upper left part of the image are also incorrectly classified as transparent.

In order to reduce the size of the incorrectly classified image area, we apply an anisotropic diffusion equation, as described in the previous section, to the variance image of Figure 2. Some computational details are as follows. The variance image is normalised so that the value of each pixel $u(\mathbf{x}) \in [0\ 1]$. Pixels of the image located outside the lens area are assigned values of 0. The gradient and divergence in eqn (1) are calculated using a central difference. Eqn (2) is solved using the semi-implicit scheme, which gives the following iteration equation:

$$L(\mathbf{x}, n+1) = \frac{\beta}{\beta+1} L(\mathbf{x}, n) + \frac{1}{\beta+1} F(\mathbf{x}, n) \tag{6}$$

where β is a ratio of the time constant, τ, and the sampling time, t_s:

$$\beta = \frac{\tau}{t_s}$$

The initial value of the diffusion matrix for each pixel, $L(\mathbf{x}, 0)$ is the 2×2 identity matrix.

We ran the anisotropic diffusion for 3×8 iteration re-

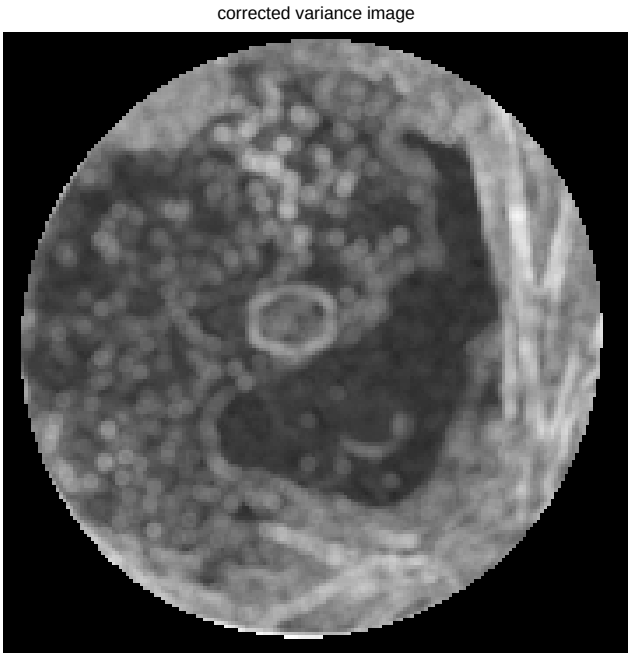

Figure 2: A corrected variance image created by a tri-directional variance operator

Figure 3: A segmented PCO image using a tri-directional variance operator

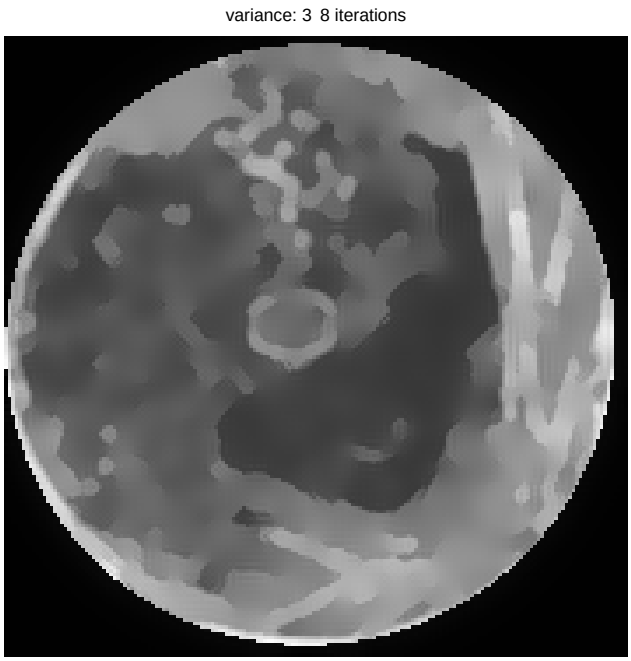

Figure 4: A post-diffusion variance image

Figure 5: A segmented PCO image after diffusion

starting the algorithm after every 8 iterations. The restarting helps to maintain the strong edges [6]. The variance image after the anisotropic diffusion is presented in Figure 4. The resulting segmented image is given in Figure 5. In comparison with the previous segmentation results (Figure 3), it can be observed that the incorrectly classified area (upper left part of the image) is significantly reduced, while the correctly classified area is unchanged.

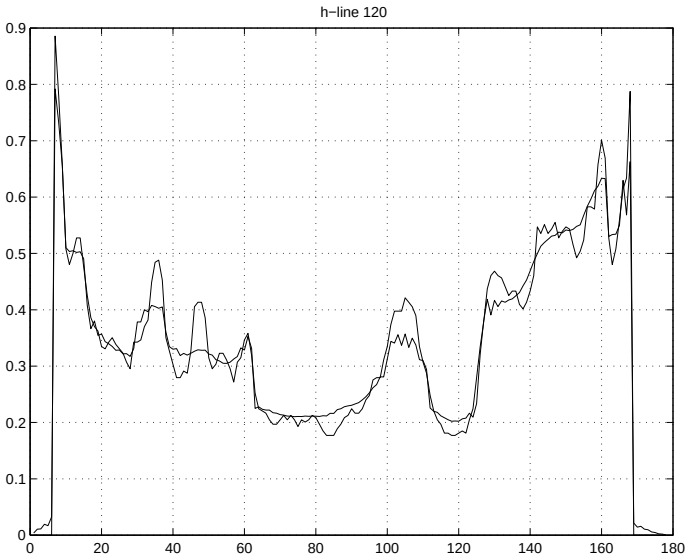

Figure 6: A cross-sectional view along a selected horizontal line of the image of Figure 4 before and after the anisotropic diffusion

A good illustration of the operation of the anisotropic diffusion equation is given in Figure 6. This is a cross-sectional view along a selected horizontal line of the image of Figure 4, before and after the diffusion. It can be noticed that the location of the strong edges characterised by large values of the gradient are preserved. Their strength is also preserved. Areas between such edges are being smoothed out. This nonlinear processing is the foundation of the anisotropic diffusion algorithm. In addition, the mean value of the image intensity (variance, in the example) is also preserved.

Concluding remarks

The anisotropic diffusion equation is one example of a rich body of variational methods which have a long history in image processing. In application to processing the PCO images, the algorithm that we study in this paper is used to improve segmentation of these images. The segmentation methods are currently based on the directional variance operator. Applying the anisotropic diffusion equation to the variance images reduces the area of incorrectly classified parts of the difficult-to-segment PCO images.

Acknowledgment

The authors would like to express their gratitude to Mr D. J. Spalton Clinical Director of the Department of Ophthalmology of St Thomas' Hospital for the specification of the problem, the provision of the image data and many useful

discussions.

References

[1] A. P. Papliński and J. F. Boyce, "Segmentation of a class of ophthalmological images using a directional variance operator and co-occurrence arrays," *Optical Engineering*, vol. 36, pp. 3140–3147, November 1997.

[2] A. P. Papliński, "Directional filtering in edge detection," *IEEE Trans. Image Proc.*, vol. 7, pp. 611–615, April 1998.

[3] A. P. Papliński and J. F. Boyce, "Co-occurrence arrays and edge density in segmentation of a class of ophthalmological images," in *Proceedings of the 4rd Conference on Digital Image Computing: Techniques and Applications, DICTA97*, (Auckland,), pp. 521–528, December 1997.

[4] A. P. Papliński and J. F. Boyce, "Tri-directional filtering in processing a class of ophthalmological images," in *Proceedings of the IEEE Region 10 Annual Conference, TENCON'97*, (Brisbane), pp. 687–690, December 1997.

[5] V. Caselles, J.-M. Morel, G. Sapiro, and A. Tannenbaum, "Introduction to the special issue on partial differential equations and geometry driven diffusion in image processing," *IEEE Transactions on Image Processing*, vol. 7, pp. 269–273, March 1998.

[6] G. H. Cottet and M. El Ayyadi, "A Voltera type model for image processing," *IEEE Transactions on Image Processing*, vol. 7, pp. 292–303, March 1998.

[7] S. T. Acton, "Multigrid anisotropic diffusion," *IEEE Transactions on Image Processing*, vol. 7, pp. 280–291, March 1998.

[8] J. Weickert and B. M. ter Haar Romney, "Efficient and reliable schemes for nonlinear diffusion filtering," *IEEE Transactions on Image Processing*, vol. 7, pp. 399–410, March 1998.

[9] A. P. Papliński and J. F. Boyce, "Processing a class of ophthalmological images using an anisotropic diffusion equation," in *Proceedings of the 2nd Annual IASTED International Conference on Computer Graphics and Imaging (CGIM'99)*, (Palm Springs, California, USA), October 1999. Accepted for presentation.

[10] A. P. Papliński and J. F. Boyce, "A first-order wave equation in modelling the behaviour of epithelial cells in an eye posterior capsule," in *Proceedings of the 6th IEEE International Workshop on Intelligent Signal Processing and Communication Systems (ISPACS'98)*, (Melbourne, Australia), November 1998.

[11] S. A. Barman, J. F. Boyce, D. J. Spalton, P. G. Ursell, and E. J. Hollick, "Measurement of posterior capsule opacification," in *Proceedings of the Conference on Medical Image Understanding and Analysis, MIUA97*, July 1997. Oxford, U.K.

[12] M. V. Pande, P. G. Ursell, D. J. Spalton, and S. Kundaiker, "High resolution digital retroillumination imaging of the posterior lens capsule after cataract surgery," *J. Cataract Refract. Surg.*, vol. 23, pp. 1521–1527, 1997.

[13] D. S. Friedman, D. D. Duncan, M. Beatriz, and S. K. West, "Digital image capture and automated analysis of posterior capsular opacification," *Invest. Ophthalmology Vis. Sci.*, vol. 40, pp. 1715–1726, July 1999.